Paper No. 95-JSC-214 Proposed for Publication in Proceedings of
5TH (1995) INTERNATIONAL OFFSHORE AND POLAR ENGINEERING CONFERENCE
The Hague, The Netherlands
June 11 - 16, 1995

SIMPLIFIED EVALUATION OF THE CAPACITIES OF TEMPLATE-TYPE OFFSHORE PLATFORMS

R. G. Bea and M. Mortazavi

Department of Civil Engineering and
Department of Naval Architecture & Offshore Engineering
University of California
Berkeley, California

ABSTRACT

During the past three decades, an immense amount of effort has been devoted to development of sophisticated computer programs to enable the assessment of storm wind, wave, and current loadings and the ultimate limit state capacity characteristics of conventional, pile-supported, template-type offshore platforms [Billington, et al., 1993; Frieze, 1993; Hellan, et al., 1993; 1994]. These programs require high degrees of expertise to operate properly, are expensive to purchase and maintain, and require large amounts of manpower and time to complete the analyses. Due to the sophistication of these programs, experience has shown that it is easy to make mistakes that are difficult to detect and that can have significant influences on the results.

This paper summarizes the second phase of development and verification of simplified procedures to evaluate environmental loadings and ultimate limit state lateral loading capacities of template-type platforms. Reasonable simplifications and high degrees of "user friendliness" have been employed in development of the software to reduce the engineering effort, expertise, and costs associated with the analyses. The computer program that has been developed to perform the simplified analyses has been identified as ULSLEA (Ultimate Limit State Limit Equilibrium Analyses) [Mortazavi, Bea, 1994].

The first phase of development and verification of these procedures has been documented [Bea, DesRoches, 1993; Bea, Craig, 1993; Bea, 1995]. The first phase developments were verified with comparisons of observed and computed loadings and capacities from five 8-pile self-contained drilling and production platforms and one 5-pile well protector. The simplified static capacity bias (nonlinear analysis capacity / simplified capacity) ranged from 0.80 to 1.03 with a mean value of 0.95. Comparisons of the computed lateral load capacities based on the simplified approach with the estimated maximum loadings sustained by these platforms during past hurricanes indicated good agreement.

During the second phase of this research, based on the experience from the first phase developments, a number of improvements were made in the simplified analyses. These improvements are detailed in this paper.

Verification of the second phase procedures is demonstrated with comparisons of the results from the advanced simplified analyses with the results from three dimensional, linear and nonlinear analyses of template-type platforms. As in the first phase, good agreement between results from the two type of analyses has been developed for the evaluations of capacities. The verification platforms include two 4-leg well protectors and one 8-leg drilling and production platform. These Gulf of Mexico platforms employed a variety of types of bracing patterns and joints. Several of these platforms were subjected to intense hurricane storm loadings during hurricanes Andrew, Camille, and Hilda. Within the population of verification platforms are several that failed or were very near failure. The simplified loading and capacity analyses are able to replicate the general performance of these platforms. Details of the nonlinear analyses of the second phase verification platforms are contained in a companion paper [Bea, Loch, Young, 1995].

INTRODUCTION

Simplified procedures have been developed to estimate the storm loadings on and lateral loading capacities of template-type offshore platforms. These procedures can be used to help screen platforms that are being evaluated for

extended service [API, 1994]. In addition, the results from these analyses can be used to help verify results from complex analytical models that are intended to determine the ultimate limit state loading capacities of platforms. Lastly, and perhaps most importantly this approach can be applied as a preliminary design tool for design of new platforms.

Using the concept of plastic hinge theory, limit equilibrium is formulated by implementing the principle of virtual work. This is the key to the simplified ultimate limit state analysis method. Where of importance, geometric and material nonlinearities are considered. This method is being increasingly used in plastic design of simple structures or structural elements (e.g. moment frames, continuous beams). Due to the impracticality of such analyses for more complicated structures, these methods have not found broad use in design or assessment of complex structures; all possible failure modes need be considered and evaluated to capture the "true" collapse mechanism and the associated ultimate lateral load.

Actual field experience and numerical results from three dimensional nonlinear analyses performed on a wide variety of template-type platforms indicate that in most cases certain failure modes govern the ultimate capacity of such platforms: plastic hinge formation in the deck legs and subsequent collapse of the deck portal, buckling of the main load carrying vertical diagonal braces in the jacket (and / or associated joint failures), lateral failure of the foundation piles due to plastic hinge formation in the piles and plastification of foundation soil, and pile pull-out or pile plunging due to exceedance of axial pile and soil capacities.

Within the framework of a simplified analysis and based on experience, collapse mechanisms are assumed for the three primary components that comprise a template-type platform: the deck legs, the jacket, and the pile foundation. Based on the presumed failure modes, the principle of virtual work is utilized to estimate the ultimate lateral capacity for each component and a profile of horizontal shear capacity of the platform is developed.

Storm intensity is based on the expected maximum wave height with wind speed and current velocities that have the same principal direction and occur at the same time as the maximum wave height. Comparison of the storm shear profile with the platform shear capacity profile identifies the "weak link" in the platform system. The base shear or total lateral loading at which the capacity of this weak link is exceeded defines the ultimate lateral capacity of the platform, R_U.

With these results, the Reserve Strength Ratio (RSR) can be determined as

$$RSR = \frac{R_U}{S_R} \tag{1}$$

S_R denotes the reference storm total maximum lateral loading.

A computer program has been developed to perform the simplified analyses based on Ultimate Limit State Limit Equilibrium Analysis (ULSLEA) techniques. Reasonable simplifications and high degrees of user friendliness have been employed in development of the software to reduce the engineering effort, expertise required, likelihood of errors, costs, and time associated with the analyses.

The remainder of this paper will detail development and verification of the advanced simplified procedures to estimate the storm loadings and ultimate limit state capacity of template-type offshore platforms.

LOADINGS AND CAPACITIES

Input Information

The geometry of the platform is defined by specifying a minimum amount of data by the user. These include the effective deck areas, the proportion and topology of jacket legs, braces, and joints, and of the foundation piles and conductors. The projected area characteristics of appurtenances such as boat landings, risers, and well conductors also must be specified. If marine fouling is present, the variation of the fouling thickness with depth may be specified by the user.

Specialized elements may be designated including grouted or ungrouted joints, braces, and legs. In addition, damaged (corrosion, holes, dents, bent, cracked) or defective elements (misalignments, under-driven piles) can be included. Dent depth and initial out-of-straightness are specified by user for braces with dents and global bending defects. User-defined element capacity reduction factors are introduced to account for other types of damage to joints, braces, and foundation elements.

Steel elastic modulus, yield strength, and effective buckling length factor for vertical diagonal braces are specified by the user. Soil characteristics are specified as the depth variation of effective undrained shear strength (for cohesive soils) or the effective internal angle of friction (for cohesionless soils). A scour depth can be specified by the user.

Storm wind speed at the deck elevation, wave height and period, current velocity profile, and storm water depth are defined by the user. These values are assumed to

be collinear and to be the values that occur at the same time. Generally, the load combination is chosen to be wind speed component and current component that occur at the same time and in the same principal direction as the expected maximum wave height. The wave period is generally taken to be expected period associated with the expected maximum wave height.

To calculate wind loadings acting on the exposed decks the user must specify the effective drag coefficient. Similarly, the user must specify the hydrodynamic drag coefficients for smooth and marine fouled members. User specified coefficients can also be introduced to recognize the effects of wave directional spreading and current blockage [API, 1993].

Environmental Loadings

Wave, current, wind, and storm tide are considered. Aerodynamic and hydrodynamic loadings are calculated according to API RP 2A guidelines [API, 1993]. The maximum wind force Sa acting on the exposed decks is based on the wind velocity pressure

$$S_a = \frac{\rho_a}{2} C_s A_d V_d^2 \qquad (2)$$

where ρ_a is the mass density of air, Cs the wind velocity pressure (drag) coefficient, Ad is the effective projected area of the exposed decks, Vd the wind velocity at the deck elevation and for an appropriate time interval.

Wave horizontal velocities are based on Stokes 5th order theory. Using equations given by Skjelbreia and Hendrickson (1961) and Fenton (1985), a computer program was developed to determine the wave kinematics (Preston, 1994). Given the wave height H, period T and water depth d, the vertical profile of maximum horizontal velocities beneath the wave crest are estimated as

$$\frac{u}{c} = K_{ds} \sum_{n=1}^{5} n\phi_n \cosh(nks) \qquad (3)$$

where K_{ds} is a coefficient that recognizes the effects of directional spreading and wave irregularity on the Stokes wave theory based velocities, k is the wave number, s is the vertical coordinate counting positive upward from the sea floor, and c is the wave celerity given as

$$\frac{C^2}{gd} = \frac{\tanh(kd)}{kd}\left[1 + \lambda^2 C_1 + \lambda^4 C_2\right] \qquad (4)$$

The crest elevation η is estimated as

$$k\eta = \sum_{n=1}^{5} \eta_n \qquad (5)$$

$\phi'n$ and $\eta'n$ are given functions of l and kd. Cn are known functions of kd only, given by Skjelbreia and Hendrickson (1961). The wave number k is obtained by implicitly solving the following equation given by Fenton(1985)

$$\frac{2\pi}{T(gk)^{0.5}} - C_0 - \left(\frac{kH}{2}\right)^2 C_2 - \left(\frac{kH}{2}\right)^4 C_4 = 0 \qquad (6)$$

The parameter λ is then calculated using the equation given by Skjelbreia and Hendickson(1961)

$$\frac{2\pi d}{gT^2} = \frac{d}{L}\tanh(kd)\left[1 + \lambda^2 C_1 + \lambda^4 C_2\right] \qquad (7)$$

The specified variation of current velocities with depth is stretched to the wave crest and modified to recognize the effects of structure blockage on the currents. The total horizontal water velocities are taken as the sum of the wave horizontal velocities and the current velocities.

The maximum hydrodynamic force, Sh, acting on the portions of structure below the wave crest are based on the fluid velocity pressure

$$S_h = \frac{\rho_w}{2} C_d A_j U^2 \qquad (8)$$

where ρ_w is the mass density of water, Aj the effective vertical projected area of the exposed structure element, and U the horizontal velocity of water at a particular point on the submerged portion of the structure element.

All of the structure elements are modeled as equivalent vertical cylinders that are located at the wave crest. Appurtenances (conductors, boat landings, risers) are modeled in a similar manner. For inclined members, the effective vertical projected area is determined by multiplying the product of member length and diameter by the cube of the cosine of its angle with the horizontal (to resolve horizontal velocities to normal to the member axis).

For wave crest elevations that reach the lower decks, the horizontal hydrodynamic forces acting on the lower decks are computed based on the projected area of the portions of the structure that would be able to withstand the high pressures. The fluid velocities and pressures are calculated in the same manner as for the other submerged portions of the structure with the exception of the definition of Cd. In recognition of rectangular shapes of the structural members in the decks a higher Cd is taken. This value is assumed to be developed at a depth equal to two velocity heads (U^2/g) below the wave crest. In recognition of the near wave surface flow distortion effects, Cd is assumed to vary linearly from its value at two velocity heads

below the wave crest to zero at the wave crest [McDonald, et al., 1990; Bea, DesRoches, 1993].

Deck Leg Shear Capacity

The ultimate shear that can be resisted by an unbraced deck portal is estimated based on bending moment capacities of the tubular deck legs that support the upper decks.

A collapse mechanism in the deck bay would form by plastic yielding of the leg sections at the top and bottom of all of the deck legs. The interaction of bending moment and axial force (M-P) is taken into account. The maximum bending moment and axial force that can be developed in a tubular deck leg is limited by local buckling of leg cross-sections.

The vertical dead loads of the decks are assumed to be equally shared between the deck legs. The vertical live loads in the deck legs caused by the lateral overturning forces are computed and summed to define the axial loading in each deck leg.

Due to relatively large axial loads (weight of the decks and topside facilities) and large relative displacements at collapse, P-Δ effect can play a role in reducing the lateral shear capacity and hence is taken into account.

To derive a realistic estimate of P-Δ effect with out leaving the framework of a simplified analysis, it is assumed that the deck is rigid. It is further assumed that plastic yielding of the sections at the bottom of the deck legs occur simultaneously, following the plastic yielding of the sections at the top of the legs and hence an estimate of plastic hinge rotations to calculate the deformations is unnecessary.

Finally, to estimate the deck bay drift at collapse Δ, the jacket is replaced by rotational springs at the bottom of each deck leg. The spring stiffness is approximated by applying external moments, which are equal in magnitude and have the same direction, to the top of jacket legs at the uppermost jacket bay. Assuming fixed boundary conditions at the bottom of these jacket legs, the rotation of cross-sections at the top of the legs and hence the rotational stiffness is determined.

The principle of virtual force is implemented to calculate the deck bay horizontal drift at collapse. Equilibrium is formulated using the principle of virtual displacement. Using the actual collapse mechanism as the virtually imposed displacement, the equilibrium equation for the lateral shear capacity of the unbraced deck portal is derived.

Jacket Bays Shear Capacity

The shear capacity of each of the bays of vertical bracing that comprise the jacket is estimated including the tensile and compressive capacity of the diagonal braces and the associated joint capacities. The capacity of a given brace is taken as the minimum of the capacity of the brace or the capacity of either its joints.

To derive a lower-bound capacity formulation, the notion of Most Likely To Fail (MLTF) element is introduced. MLTF element is defined as the member with the lowest capacity over stiffness ratio. The lower-bound lateral capacity of a jacket bay is estimated by adding the horizontal force components of all load carrying members in the given bay at the instant of first member failure. A linear multi-spring model is used to relate the forces and displacements of diagonal braces within a bay. The axial force in the jacket legs due to lateral overturning moment is estimated at each bay and its batter component is added to the lateral capacity.

An upper-bound capacity is also formulated for each bay. After the MLTF member in compression reaches its axial capacity, it can not maintain the peak load and any further increase in lateral displacement will result in unloading of this member. Presuming that the load path remains intact (inter-connecting horizontals do not fail), a load redistribution follows and other members carry the loading of the lost members until the last brace reaches its peak capacity.

An empirical residual capacity modification factor α, is introduced. Assuming elasto-perfectly plastic material behavior, α is equal to 1.0 for members in tension (neglecting strain hardening effects) and less than 1.0 for members in compression due to P-Δ effects (generally, in the range of 0.15 to 0.50). The upper-bound capacity of a given jacket bay is estimated by adding the horizontal component of the residual strength of all of the braces within the bay.

Within the framework of a simplified analysis, the jacket has been treated as a trusswork. Plastic hinge formation in the jacket legs is not considered because this hinge development occurs at a lateral deformation that is much greater than is required to mobilize the axial capacities of the vertical diagonal braces. At the large lateral deformations required to mobilize the lateral shear capacities of the legs, the diagonal brace load capacities have decreased markedly due to column buckling or tensile rupture.

In general, the effect of bending moment along the jacket legs on the lateral capacity is neglected. This leads to estimates of lateral capacity that are either conservative or

unconservative depending on the actual bending moment distribution in the legs. However, the difference in capacities (estimated vs. actual) is negligible for all but the uppermost and lowest jacket bays. Due to frame action in the deck portal and rotational restraint of the legs at mud level, the jacket legs experience relatively large bending moments at these two bays. The bending moment in the legs at the lowest bay has the direction of a resisting moment and hence not considering it can only be conservative. In contrary, the shear force due to the large moment gradient at the uppermost jacket bay has the same direction as the global lateral loading and hence reduces the lateral capacity. If this effect is not taken into account, the lateral capacity will be over-estimated.

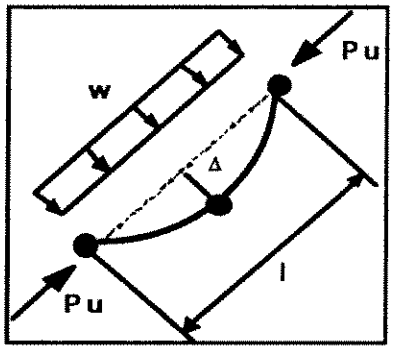

FIGURE 1: THREE HINGE FAILURE MODE FOR DIAGONAL BRACES

A simplified procedure is developed to account for the effect of shear force in the top jacket bay. We are interested in moment distribution along the legs at this bay due to frame action in the deck portal. Given the geometry of the deck portal and the load acting on deck areas, the moment distribution along the deck legs is estimated. Thinking of a jacket leg as a continuous beam which is supported by horizontal framing, the applied moment at the top of the leg rapidly decreases towards the bottom. Based on geometry of the structure, in particular jacket bay heights and the cross-sectional properties of the jacket leg (if non-prismatic), and in the limiting case of rigid supports, an upper-bound for the desired moment distribution is estimated.

The braces are treated as though there are no net hydrostatic pressures (e.g. flooded members). Based on a three-hinge failure mode, the exact solution of the second order differential equation for the bending moment of a beam-column is implemented to formulate the equilibrium at collapse (Fig. 1)

$$M_U = \left(\frac{1}{1+2\frac{\sin 0.5\varepsilon}{\sin\varepsilon}}\right)\frac{1}{\varepsilon^2}\left(\frac{1}{\cos\frac{\varepsilon}{2}}-1\right)\left(wl^2+8P_U\Delta_0\right) \tag{9}$$

$$\varepsilon = l\sqrt{\frac{P_U}{EI}} \tag{10}$$

Elasto-perfectly plastic material behavior is assumed. The ultimate compression capacity is reached when full plastification of the cross-sections at the member ends and mid-span occurs. It is further assumed that plastic hinges at member ends form first followed by plastic hinge formation at mid-span. M-P interaction condition for tubular cross-sections provides a second equation for the unknown ultimate moment M_U and axial force P_U in plastic hinges at collapse

$$\frac{M_U}{M_P} - \cos\left(\frac{\pi}{2}\frac{P_U}{P_P}\right) = 0 \tag{11}$$

The results have been verified with results from the nonlinear finite element program USFOS [Hellen, et al., 1993; 1994]. Using the same initial out-of-straightness Δ_0 for both simplified and complex analyses, the axial compression capacity of several critical diagonal members of different structures has been estimated. The simplified method slightly over-predicts the axial capacity of compression members (less than 10%).

Given the conservative formulation of buckling capacities when compared with test data (refer to Commentary D in API RP 2A-LRFD guidlines) [1993], this overprediction may in fact be closer to the expected or best estimate capacity.

The initial out-of-straightness Δ_0 is used to calibrate the axial compression capacity of braces to the column buckling curves according to API RP 2A-LRFD

$$\Delta_0 = \frac{M_P\cos\left(\frac{\pi}{2}\frac{P_{cr}}{P_P}\right)}{\left(\frac{1}{1+2\frac{\sin 0.5\varepsilon}{\sin\varepsilon}}\right)\frac{1}{\varepsilon^2}\left(\frac{1}{\cos\frac{\varepsilon}{2}}-1\right)\left(8P_{cr}\right)} \tag{12}$$

Using appropriate buckling length factors, the calibrated results are in good agreement with results from USFOS [Hellen, et al., 1994].

In case of dent damaged braces or braces with global bending damage, the axial capacity is reduced according to the equations given by Loh [1993] which were

developed for evaluating the residual strength of dented tubular members. The unity check equations have been calibrated to the lower bound of all existing test data. The equations cover axial compression and tension loading, in combination with multi-directional bending with respect to dent orientation.

Tubular Joint Capacity

The stress analysis of the circular tubular joints and the theoretical prediction of their ultimate strength has proven to be difficult. Hence, empirical capacity equations based on test results have often been used to predict the joint ultimate strength. For simple tubular joints with no gussets, diaphragms, or stiffeners, the capacity equations given in Table 1 are used.

TABLE 1: CAPACITY EQUATIONS FOR SIMPLE TUBULAR JOINTS

Joint Type	Tension	Compression
T , Y	$\frac{f_y T^2(3.4+19\beta)}{\sin\Theta}$	$\frac{f_y T^2(3.4+19\beta)}{\sin\Theta}$
DT , X	$\frac{f_y T^2(3.4+19\beta)}{\sin\Theta}$	$\frac{f_y T^2(3.4+13\beta)}{\sin\Theta} Q_\beta$
K	$\frac{f_y T^2(3.4+19\beta)}{\sin\Theta} Q_g$	$\frac{f_y T^2(3.4+19\beta)}{\sin\Theta} Q_g$

Q_b is a factor accounting for geometry and Q_g is a gap modifying factor and are estimated according to the following equations

$$Q_g = 1.8 - 0.1\frac{g}{T} \quad \text{for } \gamma \le 20 \tag{13}$$

$$Q_g = 1.8 - 4\frac{g}{D} \quad \text{for } \gamma > 20 \tag{14}$$

$$Q_\beta = \frac{0.3}{\beta(1-0.833\beta)} \quad \text{for } \beta > 0.6 \tag{15}$$

$$Q_\beta = 1.0 \quad \text{for } \beta \le 0.6 \tag{16}$$

g denotes the gap between branches of K-joints, $b = d/D$ and $g = d/2T$. d, D, and T are the branch and chord diameter and thickness respectively.

It is generally recognized that these equations for joint capacity are conservative. Bias factors (true capacity / nominal or guideline capacity) are provided in ULSLEA so that the user can utilize the expected or best estimate capacities of the elements to determine the capacity of the platform components (deck legs, jacket, foundation).

Pile Lateral Capacity

The pile shear capacity is based on an analysis similar to that of deck legs with the exception that the lateral support provided by the foundation soils and the batter shear component of the piles are included.

For **cohesive soils**, the distribution of lateral soil resistance along the pile per unit length, p_s, is assumed as

$$p_s = 9\, S_u D \tag{17}$$

where S_u is the "effective" undrained shear strength of the soil and D is the pile diameter. The effective undrained shear strength takes into account factors such as sampling or in situ testing, laboratory testing, strain rate, cyclic degradation, soil plastification and aging effects [API, 1993, 1994].

Here again, it is recognized that the traditional lateral bearing coefficient of 9 is conservative for static loadings; values in the range of 12 to 15 are more representative of the expected value. Thus, a user determined bias factor must be introduced to develop an unbiased estimate of the lateral capacity.

For a given scour depth, X, the ultimate lateral force that can be developed at the pile top is estimated as

$$P_u = 0.5\left\{-\left(27D^2S_u + 18S_uXD\right) + \left[\left(27D^2S_u + 18S_uXD\right)^2 + 144S_uDM_p\right]^{0.5}\right\} \tag{18}$$

M_p is the plastic moment capacity of the pile cross-section computed in the same manner as for the deck legs.

For **cohesionless soils**, the distribution of lateral soil pressure along a pile at a depth, z, is assumed as

$$p_s = 3\gamma z K_p \tag{19}$$

where

$$K_p = \tan^2\left(45 + \frac{\phi}{2}\right) \tag{20}$$

ϕ is the "effective" angle of internal friction of the soil and γ is the submerged unit weight of the soil. The effective angle of internal friction must take into account the same factors as cited earlier for cohesive soil conditions.

The ultimate lateral force that can be developed at the pile top with no scour is

$$P_u = 2.382\, M_p^{2/3} (\gamma D K_p)^{1/3} \qquad (21)$$

For a scour depth equal to X, the ultimate lateral force is

$$P_u' = \frac{2M_p}{\left[X + 0.544\left(\frac{P_u}{\gamma D K_p}\right)\right]^{0.5}} \qquad (22)$$

The horizontal batter component of the pile top axial loading is added to estimate the total lateral shear capacity of the piles. This component is computed based on axial loads carried by the piles due to storm force overturning moment.

Pile Axial Capacity

The axial resistance capacity of a pile is based on the combined effects of a shear yield force acting on the lateral surface of the pile and a normal yield force acting over the entire base end of the pile [API, 1993, 1994]. Thus, the ultimate axial capacity Q, is expressed as

$$Q = Q_s + Q_p = q\, A_p + f_{av} A_s \qquad (23)$$

Q_p denotes the ultimate end bearing and Q_S is the ultimate shaft capacity, q is the normal end yield force per unit of pile-end area acting on the area of pile tip A_p, and f_{av} denotes the ultimate average shear yield force per unit of embedded shaft surface area of the pile A_s.

It is assumed that the pile is rigid and that shaft friction and end bearing forces are activated simultaneously. Correction factors can be introduced to recognize the effects of the pile shaft flexibility [API, 1993, 1994].

It is further assumed that the spacing of the piles is sufficiently great so that there is no interaction between the piles (spacing to diameter ratios exceed approximately 3). In the case of compressive loading, the weight of the pile and the soil plug (for open-end piles) is deducted from the ultimate compressive loading capacity of the pile. For open-end piles, the end bearing capacity is assumed to be fully activated only when the shaft frictional capacity of the internal soil plug exceeds the full end bearing.

For **cohesive soils** with an undrained shear strength S_u, the ultimate bearing capacity is taken as the end bearing of a pile in clay

$$q = 9 S_u \qquad (24)$$

The ultimate shaft friction is taken as

$$f_{av} = \alpha S_{u,av} \qquad (25)$$

where α is the side resistance factor and a function of the average undrained shear strength $S_{u,av}$ as given in Table 2.

TABLE 2: SHAFT RESISTANCE FACTOR FOR COHESIVE SOILS

$S_{u,av}$ (ksf)	α
<0.5	1
0.5 - 1.5	1 - 0.5
>1.5	0.5

For **cohesionless soils** the ultimate bearing capacity of a deeply embedded pile is estimated as

$$q = N_q \sigma_v' \qquad (26)$$

N_q is a bearing capacity factor and a function of the friction angle of the soil Φ, and σ_v' denotes the effective pressure at the pile tip. Since sand soils possess high permeability, the pore water quickly flows out of the soil mass and the effective stress is assumed equal to applied stress. The unit shaft resistance on pile increment is estimated as

$$f_i = k\, \sigma_{vi}' \tan\delta \qquad (27)$$

where k is an earth lateral pressure coefficient assumed to be 0.8 for both tension and compression loads, σ_{vi}' denotes the effective overburden pressure at the given penetration, and δ denotes the friction angle between the soil and pile material and is taken as

$$\delta = \Phi - 5^\circ \qquad (28)$$

The unit shaft resistance and the unit end bearing capacity can not indefinitely increase with the penetration. The ultimate axial capacity of piles in cohesionless soils is estimated based on commonly used limiting values for N_q, q_{max} and f_{max} given by Focht and Kraft (1986), (Table 3).

TABLE 3: LIMITING VALUES FOR COHESIONLESS SOILS

Φ	N_q	q_{max}(ksf)	f_{max}(ksf)
20	8	40	1.0
25	12	60	1.4
30	20	100	1.7
35	40	200	2.0

PLATFORM VERIFICATIONS

Thorough analysis and verification studies on three Gulf of Mexico (GOM) Platforms have been performed [Bea, Loch, Young, 1995]. The characteristics of these structures are summarized in this section. The verification cases include two eight-leg and one four-leg drilling and production platforms. The simplified estimates of total forces acting on the platforms during intense storms and predictions of ultimate member strength and platform capacity were verified with results from complex nonlinear analyses [Bea, Loch, Young, 1995].

In the case of platform "A", the results available from a detailed nonlinear push-over analysis were used to verify the simplified analysis' results [Bea, DesRoches, 1993; Bea, 1995]. In the case of platforms "B" and "C", the nonlinear finite element computer program USFOS was utilized to perform the static push-over analyses. Wave and wind loads in the deck were calculated and applied as nodal loads. The hydrodynamic forces on jacket were generated using the WAJAC wave load program [Det Norske Veritas, 1993]. Stokes 5th order wave theory was used and member loads were calculated based on the Morison, Johnson, O'Brien, and Schaff (MJOS) equation [API, 1993].

Simplified analyses were performed assuming elasto-perfectly plastic behavior for members in both tension and compression (a residual strength factor of α=1.0) to estimate the upper-bound capacities of jacket bays.

Platform "A" is an 8-leg structure located in the Main Pass area of the Gulf of Mexico in a water depth of 271 feet. Designed and installed in 1968-70, the platform has been exposed to high environmental loading developed by hurricanes passing through the Gulf. The structure foundation consists of eight 42-inch piles which penetrate to a depth of 270 ft into medium sands overlaying stiff clays. The jacket legs are battered in two directions and the leg-pile annulus is grouted. The lower and upper decks are located at +46 ft and +63 ft respectively.

The detailed nonlinear analysis was performed using a 9th order Stream Function to compute wave crest elevations. A wave steepness of 1/12 was used (wave period of 12.8 seconds for the 100-year wave). Marine growth on the platform was taken as having an average thickness of 1 in. and considered for all members located between the waterline and -100 ft.

The MJOS equation was used to compute the local forces on members. The drag coefficient was taken as Cd = 1.2 and the inertia coefficient was taken as Cm = 1.2. Wind forces were computed using the API RP 2A formulation assuming a drag coefficient of Cs = 1.0 for clear decks, 1.5 for cluttered and 2.0 for blocked decks.

The wave crest begins to impact the deck at about the 100-yr. return period storm condition. The additional forces due to deck inundation were calculated as previously described. The wave impact loads were computed using full impact area and a drag coefficient of Cd = 2.0. The remaining deck area not covered by the wave is exposed to the wind. This wind forces were calculated and added to the wave forces.

The ULS lateral loading capacities were determined for the platform's principal orthogonal directions. In the case of end-on loading, the wave in deck condition resulted in an ultimate lateral load capacity of 2,600 kips. Most of the member failures were due to compressive buckling of braces. The analyses indicated a brittle strength behavior and little effective redundancy which is a typical result for K-braced platform systems [Bea, DesRoches 1993; Bea, 1995]. In the case of broadside loading with wave in the deck, the ultimate capacity was 2,940 kips.

The same oceanographic conditions and hydrodynamic coefficients utilized in the detailed analysis were used to perform a simplified analysis. For 100 year storm conditions, the simplified analysis indicated 3,400 kips and 2,900 kips total base shear for broadside and end-on loading, respectively (Figs. 2 and 3).

Compared with the results from detailed analysis, the total base shear is over-predicted by less than 15 %. The principal difference is due to modeling assumptions in the simplified analysis: all of the platform elements are modeled as equivalent vertical cylinders that are concentrated at a single vertical position in the wave crest.

The platform shear capacities and storm shears (abscissa) are plotted versus platform elevation (ordinate, above, +, below, -, mean sea level) in Figs. 2 and 3. In broadside loading, ULSLEA predicted a failure mode in the

second jacket bay at a total base shear of about 3,400 kips. In end-on loading, ULSLEA indicated a failure due to buckling of compression braces in the uppermost jacket bay at a lateral load of 2,900 kips (Fig. 3).

These results are 10 to 15% higher than those gained from detailed nonlinear analyses. The principal difference lies in the nonlinear modeling of vertical diagonal braces which results in different buckling loads.

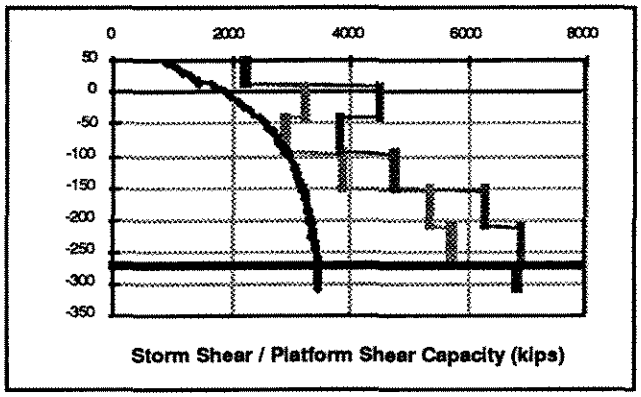

FIGURE 2: PLATFORM "A" BROADSIDE STORM SHEARS AND PLATFORM SHEAR CAPACITIES

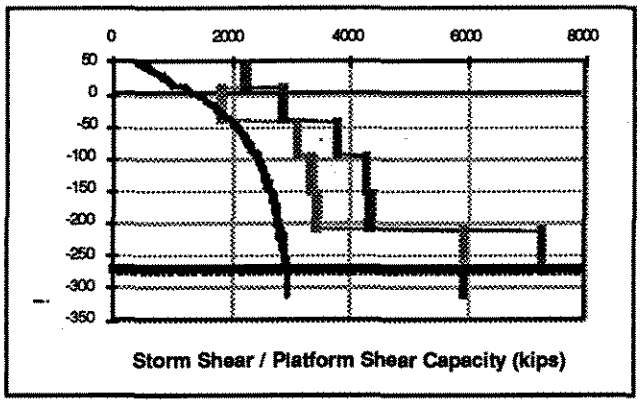

FIGURE 3: PLATFORM "A" END-ON STORM SHEARS AND PLATFORM SHEAR CAPACITIES

Platform "B" is an eight-leg structure located in a water depth of 118 ft [Imm, et al., 1994]. The platform was designed using a design wave height of 55 ft. The cellar and main decks are located at +34 ft and +47 ft, respectively. The 39 in. jacket legs are battered in two directions and have no joint cans. The 36 in. piles are grouted inside the jacket legs.

Nonlinear push-over analysis results indicated that the platform is capable of resisting approximately 3,850 kips in broadside loading [Bea, Loch, Young, 1995; Imm, et al., 1994]. The failure mechanism occurs in the uppermost jacket bay due to buckling of the compression braces. The analysis indicates a brittle strength behavior and no effective redundancy. The analysis showed the platform's end-on resistance capacity to be approximately 3,900 kips. Failure begins in the uppermost jacket bay, where the four diagonal compression braces buckle almost simultaneously. The failure mechanism is completed when the horizontal struts in the upper jacket bay buckle in addition to compression braces.

The same oceanographic conditions, hydrodynamic coefficients, and wave theory (Stokes 5th order) utilized in nonlinear push-over analyses were used to perform an ULSLEA. Since the same procedure was used to estimate the wind and wave forces on the projected deck areas, they were essentially the same for both detailed and simplified analyses. The resulting storm shears are summarized in Figs. 4 and 5.

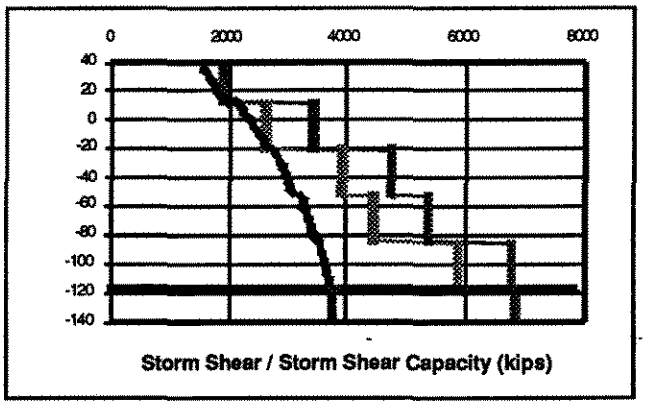

FIGURE 4: PLATFORM "B" BROADSIDE STORM SHEARS AND PLATFORM SHEAR CAPACITIES

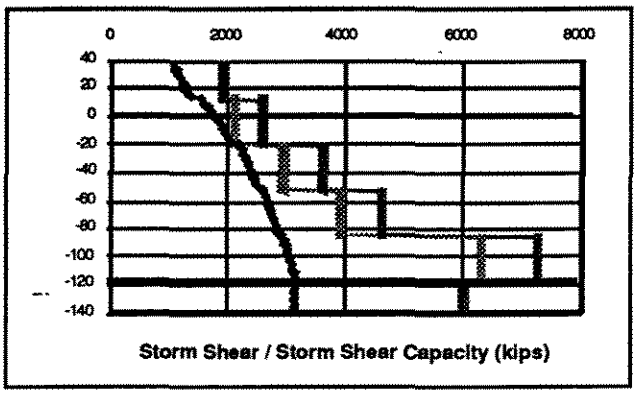

FIGURE 5: PLATFORM "B" END-ON STORM SHEARS AND PLATFORM SHEAR CAPACITIES

In broadside loading direction, the simplified force calculation procedures over-estimated the hydrodynamic loads on the jacket by 7 %. In end-on loading direction, the jacket loads were over-estimated by 15 %.

For each loading direction, the predicted performance of MLTF vertical diagonal brace has been verified. Using the same initial out-of-straightness for both simplified and complex analyses, the simplified column buckling formulation over-predicted the peak member load by 6 % and 9 % for end-on and broadside loading directions respectively. Using the calibrated format of simplified column buckling equations with a buckling length factor of K=0.65, the simplified analysis under-predicted the peak load by 7 % and 1 % for end-on and broadside loading directions respectively.

To study the effect of K-factor on predicted buckling load, a sensitivity analysis was performed. The calibrated buckling capacity formulation gave the "exact" result when buckling length factors of K=0.65 and 0.55 were used for MLTF members in compression for broadside and end-on loading directions respectively. Note that in the latter case, the brace is connected to jacket legs at both ends and is therefore stiffer. It is interesting to note that this result is in good agreement with those presented by Hellan, et al. (1994).

The platform shear capacity and storm shear profiles are plotted versus platform elevation in Figs. 4 and 5. In case of broadside loading and using a buckling length factor of K=0.65 for braces in compression, ULSLEA predicts a failure mode in the deck legs and uppermost jacket bay at a total base shear of about 3,600 kips, which is in good agreement with the results from non linear analysis (~ 6 % under-prediction). In case of end-on loading with a buckling length factor of K=0.55 for compression braces, the simplified analysis predicts a collapse load of 3,100 kips (~ 20 % under-prediction) due to failure of compression braces in the top jacket bay.

Platform "C" is a self contained four pile well protector. It was installed in the Gulf of Mexico Ship Shoal region in a water depth of 157 ft in 1971. The platform has four decks at elevations +33 ft, +43 ft, +56 ft, and +71 ft. The jacket legs are battered in two directions and have joint cans. The leg-pile annulus is ungrouted and the piles attached to the jacket with welded shimmed connections at the top of the jacket.

This platform has been the subject of extensive structural analyses [PMB Engineering Inc., 1994]. As part of an industry wide effort to assess the variability in predicted performance of offshore platforms in extreme storms, the storm loadings and ultimate capacity of this platform has been assessed by many investigators using a variety of nonlinear analysis software packages. All of the analysists were given the same platform drawings, soil conditions, and oceanographic conditions. It was specified that the storm loadings should be computed according to API guidelines [API, 1993, 1994]. It is noteworthy that the range of RSR's determined in this study varied from 0.5 to 2.5; a range of 5. Such a range in the results from the nonlinear analyses makes the differences between the results obtained from ULSLEA and those from the complex nonlinear analyses (USFOS) seem very small.

As part of the companion study documented by Bea, et al. [1995], platform "C" was analyzed using USFOS. As for all of the nonlinear analyses, an attempt was made to use "unbiased" characterizations for all loading and capacity factors to develop best estimate lateral loadings and capacities. The results from the USFOS analyses of platform "C" indicated a maximum total lateral loading of 2,900 kips and a lateral capacity of 1,670 kips to 3,440 kips. The range in lateral capacity was a function of how the foundation piles were modeled. If "static" capacities were utilized, the initiating failure mode was in the foundation and the lower lateral loading capacity resulted. If "dynamic" capacities were utilized, the initiating failure mode was in the jacket and the upper lateral loading capacity resulted. As found in previous analyses [Bea, DesRoches, 1993; Bea, Craig, 1994; Bea, 1995], the methods used model the performance characteristics of the pile foundations can have marked effects on the platform lateral loading capacity.

Using the simplified approach for a reference wave height of 67 ft, a wave period of 14.3 sec and a uniform current velocity of 3.1 ft/sec, the total base shear for an orthogonal loading direction was estimated to be 3,050 kips (Fig. 6). Using a buckling length factor of 0.65 for compression braces, ULSLEA indicated platform collapse at a base shear of 3,200 kips due to simultaneous failure of compression braces at three different jacket bays. For this lateral loading, the mean axial pile static capacity in compression was exceeded by approximately 30 % (RSR = 0.7). According to this "best estimate" result, a failure mode in foundation would govern the ultimate capacity of the platform. However, recognition of dynamic loading effects in the foundation indicated that the failure mode would be in the jacket rather than in the pile foundation.

These results are in good agreement with those gained from detailed nonlinear analysis. The comparison indicated that the simplified method over-estimated the current and wave loads in jacket by 17 %. The ultimate capacity of the platform with the dynamic pile foundation characteristics was under-predicted by 6 %. The axial com-

pression capacity of piles were over-estimated by 14 %. After including the self-weight of the jacket to the axial pile loading, the pile capacities were in close agreement. Due to how the piles are installed and the potential loadings carried by the mudline braces and mudmats, whether or not the dead loads are actually carried by the supporting piles is uncertain.

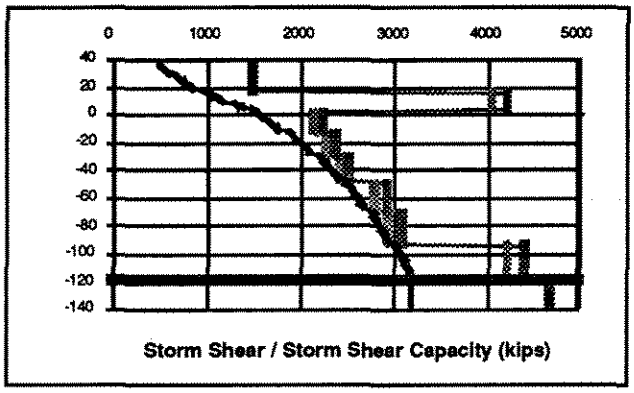

FIGURE 6: PLATFORM "C" STORM SHEARS AND PLATFORM SHEAR CAPACITIES (DYNAMIC FOUNDATION CONDITION)

SUMMARY AND CONCLUSIONS

Simplified procedures are presented to evaluate the structural performance of template-type platforms under extreme storm conditions. The results summarized in Table 4 and those given earlier by Bea and DesRoches (1993), Bea and Craig [1994], and Bea [1995] indicate that ULSLEA can develop evaluations of both storm loadings on and ultimate lateral capacities of platforms that are excellent approximations of those derived from complex analyses.

Comparison of the estimated lateral load capacities with the estimated maximum loadings that these platforms have experienced and with observed performance characteristics of these platforms indicates that the analytical evaluations of both storm loadings and platform capacities are also in good agreement with the experience.

The use of the simplified analytical procedures to estimate reference storm lateral loading and platform capacities, and Reserve Strength Ratios are indicated to result in good estimates that can be used in the process of screening platforms that are being evaluated for extended service. In addition, the results from these analyses can be used to help verify results from complex analytical models that are intended to determine the ultimate limit state loading capacities of platforms. Lastly, this approach can be applied as a preliminary design tool for configuration of new platforms.

CONTINUING WORK

This study is part of a multi-year joint industry - government sponsored research project to develop simplified methods to analyze the static and dynamic ultimate limit state performance characteristics of platforms. At the present time, detailed nonlinear analyses are being performed on two additional 8-leg platforms that were subjected to storm loadings by hurricane "Andrew" [Botelho, et al., 1994; Petrauskas, et al., 1994]. One of these seemingly identical 8-leg platforms failed and the other did not. Similar detailed nonlinear analyses have been performed on two apparently identical 4-pile well protectors that also were subjected to loadings from hurricane Andrew [Bea, Loch, Young, 1995]. Again, one of these well protectors failed while the other did not. As detailed in a companion paper [Bea, Loch, Young, 1995], the difference in observed performance can be explained in the subtle differences between these platforms. Verification of ULSLEA with these results will be the subject of future publications.

ACKNOWLEDGMENTS

The results summarized in this paper have been developed as a result of a series of joint industry - government sponsored projects conducted by the Marine Technology Development Group the University of California during the past three years. Appreciation is expressed to the sponsors including Arco Exploration Co., Exxon Production Research Co., UNOCAL Corp., Shell Oil Co., Mobil Research and Development Co., the U. S. Minerals Management Service, the California State Lands Commission, and the California and National Sea Grant College Programs. Support and assistance have also been provided by Chevron Petroleum Technology Co., and Amoco Production Co.

This paper is funded in part by a grant from the National Sea Grant College Program, National Oceanic and Atmospheric Administration, U. S. Department of Commerce, under grant number NA89AA-D-SG138, project numbers R/OE-11 and R/0E-19 through the California Sea Grant College, and in part by the California State Resources Agency. The views expressed herein are those of the authors and do not necessarily reflect the views of NOAA or any of its sub-agencies. The U. S. Government is authorized to reproduce and distribute for governmental purposes.

TABLE 4: COMPARISON OF USFOS AND ULSLEA RESULTS

Platform	Configuration	Wave Direction	ULSLEA		USFOS		Ratio USFOS/ULSLEA
			Failure Mode	Base Shear (kips)	Failure Mode	Base Shear (kips)	
A	8 leg double battered K-braced	End-on Broadside	1st jacket bay 2nd jacket bay	2,900 3,400	1st jacket bay 2nd jacket bay	2,600 2,930	0.9 0.86
B	8 leg double battered K-braced	End-on Broadside	deck legs & 1st jacket bay 1st jacket bay	3,130 3,670	1st jacket bay 1st jacket bay	3,900 3,860	1.25 1.05
C	4 leg double battered K-braced	End-on End-on	4th , 5th and 6th jacket bays Foundation	3,210 1,950 (1,740)	5th and 6th jacket bays Foundation	3,440 1,670	1.07 0.86 (0.96)*

*) Including the platform selfweight

REFERENCES

American Petroleum Institute (API), 1993. "Recommended Practice for Planning, Designing and Constructing Fixed Offshore Platforms - Load and Resistance Factor Design (RP 2A-LRFD)," First Edition, July, Washington, D. C.

American Petroleum Institute, 1994. "API RP 2A-WSD 20th Edition, Draft Section 17.0, Assessment of Existing Platforms," November, Houston, Texas.

Bea, R. G., and DesRoches, R., 1993, "Development and Verification of A Simplified Procedure to Estimate The Capacity of Template-Type Platforms," *Proceedings 5th International Symposium Integrity of Offshore Structures*, D. Faulkner et al., Emas Scientific Publications, pp. 129-148.

Bea, R. G., and Craig, M. J. K. 1993. "Developments in the Assessment and Requalification of Offshore Platforms." Proceedings Offshore Technology Conference, OTC 7138, Houston, Texas, May.

Bea, R. G.. 1995. "Development & Verification of a Simplified Method to Evaluate Storm Loadings on and Capacities of Steel, Template-Type Platforms." *Proceedings Energy & Environmental Expo 95*, American Society of Mechanical Engineers, Houston, Texas, Jan.

Bea, R. G., Loch, K., Young, P. 1995. "Evaluation of Capacities of Template-Type Gulf of Mexico Platforms." *Proceedings 5th International Offshore and Polar Engineering Conference, ISOPE-95*, The Hague, The Netherlands, June.

Billington, C. J., Bolt, H. M., and Ward, J. K. 1993. "Reserve, Residual and Ultimate Strength Analysis of Offshore Structures: State of the Art Review." Proceedings Third International Offshore and Polar Engineering Conference, Singapore, June, pp. 125-133.

Botelho, D. L. R., Petrauskas, C., Mitchell, T. J., and Kan, D. K. Y. 1994. "A Detailed Study on the Failure Probability of ST 130 'A' Platform During the Passage of Hurricane Andrew." Proceedings Offshore Technology Conference, OTC 7473, Houston, Texas, May.

Det Norske Veritas. 1993. "WACJAC, Wave and Current Loads on Fixed Rigid Frame Structures." SESAM AS, Version 5.4-02, Oslo, Norway.

Fenton, J. D., 1985, "A Fifth Order Stokes Theory for Steady Waves," *Journal of Waterway, Port, Coastal and Ocean Engineering*, American Society of Civil Engineers, Vol. 111, No. 2, pp. 216-234.

Focht, J. A., and Kraft, L. M., 1986, "Axial Performance and Capacity of Piles," *Planning and Design of Fixed Offshore Platforms*, McClelland, B., and Reifel, M. D., pp. 763-801.

Frieze, P.A. 1993. "Determination of Platform Overall Reliability Given Reserve Strength Ratio (RSR)." Report to Health and Safety Executive, Report PAFA 012/1, London, April.

Hellan, O., et al. 1993. "Nonlinear Re-Assessment of Jacket Structures Under Extreme Storm Cyclic

Loading." Proceedings of the Offshore Mechanics and Arctic Engineering Conference, Glasgow, Scotland.

Hellan, O., et al., 1994, "Use of Nonlinear Pushover Analyses in Ultimate Limit State Design and Integrity Assessment of Jacket Structures," *Proceedings, Offshore Mechanics and Arctic Engineering, OMAE '94.*

Imm, G. R., O'Connor, J. M., Light, J. M., and Stahl, B. 1994. "South Timbalier 161A: A Successful Application Platform Requalification Technology." *Proceedings Offshore Technology Conference,* OTC 7471, Houston, Texas, May.

Loh, J. T., 1993, "Ultimate Strength of Dented Tubular Steel Members," *Proceedings, 3rd International Offshore and Polar Engineering Conference, Singapore.*

McDonald, D. T., Bando, K.,, Bea, R. G., Sobey, R. J. (1990). "Near Surface Wave Forces on Horizontal Members and Decks of Offshore Platforms, Final Report," Coastal and Hydraulic Engineering, Dept. Of Civil Engrg., Univ. Of California at Berkeley, Dec.

Petrauskas, C., Botelho, D. L. R., Krieger, W. F., and Griffin, J. J. (1994). "A Reliability Model for Offshore Platforms and its Application to ST151 "H" and "K" Platforms During Hurricane Andrew (1992)," Proceedings of the Behavior of Offshore Structure Systems, Boss'94, Massachusetts Institute of Technology.

Mortazavi, M. and Bea, R. G. (1994). "ULSLEA, Simplified Nonlinear analysis for Offshore Structures," Report to Joint Industry - Government Sponsored Project, Marine Technology Development Group, University of California at Berkeley, June.

PMB Engineering Inc. (1994). "Benchmark Analysis, Trial Application of the API RP 2A-WSD Draft Section 17," Report to Minerals Management Service and Trials JIP Participants, Sept.

Preston, D., 1994, "An Assessment of the Environmental Loads on the Ocean Motion International Platform," MS Thesis, Department of Naval Architecture and Offshore Engineering, University of California, Berkeley.

Skjelbreia, L., and Hendrickson J., 1961, "Fifth Order Gravity Wave Theory," Proceedings, 7th Conference of Coastal Engineering, pp. 184-196.